Inorganic Chemistry

Article

pubs.acs.org/IC

Coordination Complexes of Bismuth Triflates with Tetrahydrofuran and Diphosphine Ligands

Saurabh S. Chitnis,[†] Neil Burford,*[,†] Andreas Decken,[‡] and Michael J. Ferguson[§]

[†]Department of Chemistry, University of Victoria, Victoria, British Columbia, Canada V8W 3V6
[‡]Department of Chemistry, University of New Brunswick, Fredericton, New Brunswick, Canada E3A 6E2
[§]Department of Chemistry, University of Alberta, Edmonton, Alberta, Canada T6G 2G2

Supporting Information

ABSTRACT: The reaction of $CH_3OSO_2CF_3$ (MeOTf) with $BiBr_3$ in tetrahydrofuran (THF) yields $(THF)_2BiBr_2(OTf)$ (**1**), which is converted to $(dmpe)BiBr_2(OTf)$ (**2Br**) upon displacement of the THF ligands with bis(dimethylphosphino)ethane (dmpe). The chloride derivatives $(dmpe)BiCl_2(OTf)$ (**2Cl**) and $(dmpe)BiCl(OTf)_2$ (**3**) are obtained from the reaction of $BiCl_3$ and dmpe with 1 and 2 equiv of $Me_3SiOSO_2CF_3$ (TMSOTf), respectively. The complexes readily decompose in solution to give elemental bismuth and a mixture of products. The solid-state structures reveal dimeric units bridged by both triflate O−S−O interactions and weak Bi−X−Bi interactions (X = Cl, Br). Comparison of the solid-state structures illustrates that both cis and trans configurations of halides are possible in complexes of the form $L_2BiX_2(OTf)$, depending upon the denticity of the ligand. The experimentally observed configurations are consistent with minima calculated at the MP2 level for the triflate-free cations in the gas phase. Examination of the MP2-calculated electronic structure of **3** reveals the presence of low-lying π-type orbitals that may result in Z-type ligand activity. However, the attempted coordination of **3** with the electron-rich metal center in K_2PdCl_4, via metal-to-ligand back-donation, leads instead to halide abstraction, giving $[(dmpe)_2Pd][(CH_3CN)_2Bi_2Cl_6(OTf)_2]$ (**8**). The anion in **8** consists of two octahedral bismuth environments bridged along one edge by two triflate anions. The results illustrate new coordination chemistry for bismuth.

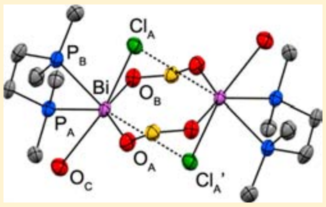

INTRODUCTION

Coordination chemistry of the p-block elements is superficially developed in comparison to that of the transition elements but offers interesting bonding features, especially for the pnictogens and chalcogens, in which it is possible for the Lewis-acidic acceptor site to also possess a lone pair of electrons. A variety of phosphine complexes of low-valent phosphorus,[1] arsenic,[2] or antimony[3−5] acceptors have recently been reported in which the Lewis acidity of the lone-pair-bearing acceptor has been enhanced by the introduction of a cationic charge, illustrating new structure and bonding and unusual redox chemistry. The analogous coordination chemistry for bismuth is evidenced only by $[(Ph_3P)_2BiPh_2][PF_6]$[6] and the spectroscopic characterization of $[Ph_3PBiPh_2][PF_6]$[6] and $[Ph_3PBiCl_2][AlCl_4]$.[7] In view of the diverse coordination chemistry that is developing for bismuth with amine donors,[8,9] and the established phosphine complexes of neutral $[Bi_2Br_6(PMe_3)_4$, $Bi_4Br_{12}(PEt_3)_4$, $Bi_2Br_6(dmpe)_2$, $Bi_2Br_6(PPhMe_2)_2(OPPhMe_2)_2$,[10] $Bi_2Cl_6(dppm)_2$, $Bi_4Cl_{12}(dppe)_5$, $Bi_2Cl_6(dppe)_3]$,[11] $[BiX_3\{o\text{-}C_6H_4(PPh_2)_2\}]$ (X = Br, I), and $[BiX_3\{o\text{-}C_6H_4(PMe_2)_2\}]$ (X = Cl, Br, I)[12] and anionic ($[Bi_2Br_7(PMe_3)_2]^-$,[13] $[BiI_4(dmpe)]^-$,[14] and $[BiI_4(PhPMe_2)]^-$[15]) bismuth halides, we have examined trifluoromethanesulfonate (triflate or OTf) derivatives of bismuth halides with the expectation of augmenting the Lewis acidity at bismuth (dmpe = 1,4-tetramethyldiphosphinoethane, dppm = 1,3-tetraphenyldiphosphinomethane, and dppe = 1,4-tetraphenyldiphosphinoethane). Here we report the synthesis and structural characterization of $(THF)_2BiBr_2(OTf)$ (**1**), $(dmpe)BiBr_2(OTf)$ (**2Br**), $(dmpe)BiCl_2(OTf)$ (**2Cl**), and $(dmpe)BiCl(OTf)_2$ (**3**). The new compounds are bismuth derivatives of recently reported antimony complexes.[3] Moreover, the compounds are analogous to the recently reported cationic ligands of the form $[LPR_2]^+$ and $[L_3P]^{3+}$ (L = carbene), in which the low-lying vacant acceptor orbitals and the lone pair at the phosphorus atom impart unusual catalytic behavior to their complexes with electron-rich late transition metals.[16−18] In this context, we have also examined the potential interaction of $\mathbf{3}(OTf)_2$ with K_2PdCl_4, leading to the dianion $[(CH_3CN)_2Bi_2Cl_6(OTf)_2]^{2-}$.

EXPERIMENTAL SECTION

Reactions were carried out in an Innovative Technologies or MBraun glovebox under an atmosphere of dry and deoxygenated N_2. Large-scale reactions were performed on a Schlenk line using standard inert-air techniques under an atmosphere of dry and deoxygenated argon. Dichloromethane (DCM), toluene, hexane, and *n*-pentane were purified on an MBraun solvent purification system. High-performance liquid chromatography grade MeCN was purchased from Aldrich and dried by distillation from CaH_2 under an atmosphere of argon. Tetrahydrofuran (THF) was distilled from sodium/benzophenone under an atmosphere of argon. All solvents were stored over freshly activated 4 Å molecular sieves. Deuterated solvents were purchased from Aldrich and dried using 4 Å molecular sieves. MeOTf (>98%) and dmpe (97%) were obtained from Aldrich and used after

Received: April 9, 2013
Published: May 29, 2013

distillation. $BiBr_3$ (Strem Chemicals, 99.999%), $BiCl_3$ (Strem Chemicals, 99.999%), and K_2PdCl_4 (Aldrich, 99.99%) were used as received. TMSOTf (99%) was purchased from Aldrich and distilled prior to use. NMR spectra were obtained at room temperature, unless otherwise stated, on a Bruker AVANCE 500 ^1H (500.13 MHz, 11.7 T) and a Bruker AVANCE 300 ^1H (300.15 MHz, 7.02 T). Chemical shifts (δ) are reported in ppm. ^{13}C (125.76 MHz) chemical shifts are referenced to δ_{TMS} = 0.00 ppm, and ^{31}P (202.46 and 121.56 MHz) chemical shifts are referenced to $\delta_{H_3PO_4\ (85\%)}$ = 0.00 ppm. Spectra were obtained in an appropriate deuterated solvent in 5 mm tubes that were capped and sealed with Teflon and Parafilm prior to removal from the inert atmosphere. Melting points were recorded on an electrothermal apparatus in sealed capillary tubes under N_2. Elemental analyses of selected samples were performed by Canadian Microanalytical Services Ltd., Delta, British Columbia, Canada. Single-crystal X-ray diffraction was carried out using either a Bruker AXS P4/SMART 1000 or a PLATFORM/APEX II CCD diffractometer under a stream of cold N_2.

Computational Details. Quantum-chemical calculations were performed using *Gaussian09*.[19] All structures were optimized without symmetry constraints at the MP2 level using the cc-pWCVDZ basis set[20] and the Stuttgart−Cologne fully relativistic ECP (ECP60MDF)[21] for bismuth. All other atoms were modeled using the cc-PVDZ basis set. Structures were characterized as true minima by analytical frequency calculations that showed zero negative frequencies.

$(THF)_2BiBr_2(OTf)$ (1). $BiBr_3$ (11.217 g, 25 mmol) was dissolved in THF (50 mL) in a Schlenk bulb and stirred to obtain a clear, golden-yellow solution. A solution of MeOTf (4.103 g, 25 mmol) in THF (12 mL) was added over 20 min through an addition funnel with an oil bubbler attached to vent CH_3Br. Gaseous evolution and a slight exotherm were observed over the course of the addition. Stirring for an additional 16 h at room temperature produced a viscous white suspension. The slurry was pumped to dryness over 16 h under a dynamic vacuum to yield a sticky light-gray solid (15.303 g). This product was recrystallized from a 1:1 (v/v) mixture of DCM/Et_2O at −30 °C over 72 h, and the shiny, translucent blocks obtained were isolated by decantation. The crystals were identified as **1** using X-ray crystallography. Because of the high degree of disorder in the THF molecules, precise bond lengths and angles could not be obtained. The identity of the bulk was established via elemental analysis and NMR spectroscopy, which confirmed that the coordinated THF molecules are not removed even after prolonged exposure to high vacuum at room temperature. Yield (crystals): 10.031 g, 78%. Mp: 108−110 °C. Elem anal. Calcd (found) for **1**: C, 15.90 (16.33); H, 2.61 (2.44). ^1H NMR (300 MHz, CD_2Cl_2, 298 K): δ 2.00 (m, 4H, *THF*), 4.15 (m, 4H, *THF*). $^{13}C\{^1H\}$ NMR (75 MHz, CD_2Cl_2, 298 K): δ 26.1 (s), 71.1 (s), 116.8 (q, CF_3, $^1J_{P-C}$ = 319.8 Hz). Raman (cm^{-1}, [relative intensity]): 84.1 [45], 93.1 [28], 191.9 [52], 212.1 [100], 322.1 [6], 346.8 [5], 352.4 [11], 519.7 [1], 578.1 [3], 763.3 [24], 854.2 [6], 922.7 [6], 1022.6 [60], 1041.7 [4], 1185.4 [4], 1224.7 [7], 1347.0 [1], 1368.4 [4], 1450.3 [4], 1487.3 [5], 2880.5 [11], 2902.9 [18], 2936.6 [19], 2954.6 [17], 2991.6 [23].

$(dmpe)BiBr_2(OTf)$ (2Br). **1** (0.662 g, 1 mmol) in toluene (5 mL) was added dropwise to a solution of dmpe (0.150 g, 1 mmol) in toluene (5 mL). A bright-yellow precipitate was obtained immediately. The reaction was allowed to stir for an additional 1 h to yield a light-gray precipitate, which was filtered and washed with pentane (3 × 5 mL). Removal of the solvent over 4 h gave a light-gray powder together with some insoluble black precipitate. The crude product was recrystallized from a minimum amount of CH_3CN at −30 °C to yield translucent blocks, which were identified as **2Br**·CH_3CN using X-ray crystallography. Yield (crystals): 0.548 g, 77%. Mp: 225 °C (dec). Elem anal. Calcd (found) for **2Br**·CH_3CN: C, 15.25 (16.54); H, 2.70 (2.65); the sample shows visible decomposition (formation of an insoluble brown/black powder) under vacuum (10^{-2} mbar) and, consequently, attempts to obtain better analytical results were unsuccessful. ^1H NMR (500 MHz, CD_3CN, 298 K): δ 2.41 (d, 12H, $\mathit{Me}_2PCH_2CH_2P\mathit{Me}_2$, $^2J_{P-H}$ = 14.5 Hz), 3.06 (m, 4H, $Me_2P\mathit{CH_2CH_2}PMe_2$). ^{31}P NMR (200 MHz, CD_3CN, 298 K): δ 50.8 (br). Raman: the sample decomposes in the laser beam.

$(dmpe)BiCl_2(OTf)$ (2Cl). A solution of dmpe (0.150 g, 1 mmol) in toluene (5 mL) was added dropwise to a suspension of $BiCl_3$ (0.316 g, 1 mmol) and TMSOTf (0.222 g, 1 mmol) in toluene (10 mL). A yellow precipitate was observed immediately. The reaction was allowed to stir for 2 h to yield a yellow precipitate under a clear and colorless supernatant, which was filtered and washed with pentane (3 × 5 mL). Removal of the solvent over 16 h yielded a fine yellow powder, which was recrystallized from a minimum amount of CH_3CN at −30 °C over 48 h to yield large crystalline blocks, identified as **2Cl**·CH_3CN using X-ray crystallography. Yield (crystals): 0.337 g, 54%. Mp: 220 °C (dec). ^1H NMR (500 MHz, CD_3CN, 298 K): δ 2.30 (d, 12H, $\mathit{Me}_2PCH_2CH_2P\mathit{Me}_2$, $^2J_{P-H}$ = 14.7 Hz), 3.10 (m, $Me_2P\mathit{CH_2CH_2}PMe_2$, 4H). $^{13}C\{^1H\}$ NMR (125 MHz, CD_3CN, 298 K): δ 9.8 (d, $^1J_{P-C}$ = 28 Hz), 31.3 (d, $^1J_{P-C}$ = 29 Hz). ^{31}P NMR (200 MHz, CD_3CN, 298 K): δ 80.7 (br). Raman: the sample decomposes in the laser beam.

$(dmpe)BiCl(OTf)_2$ (3). A solution of dmpe (0.150 g, 1 mmol) in toluene (10 mL) was added dropwise to a suspension of $BiCl_3$ (0.316 g, 1 mmol) and TMSOTf (0.444 g, 2 mmol) in toluene (10 mL). A yellow precipitate was observed immediately. The reaction was allowed to stir for 1 h to yield a yellow suspension. The product was filtered and washed with pentane (3 × 5 mL). Removal of the solvent over 24 h yielded a fine yellow powder, which was recrystallized from a minimum amount of CH_3CN at −30 °C to yield colorless crystalline blocks, identified as dmpeBiCl(OTf)$_2$·CH_3CN using X-ray crystallography. Yield (crystals): 0.496 g, 68%. Mp: 207−212 °C (dec). Elem anal. Calcd (found) for **3**·CH_3CN: C, 16.37 (16.20); H, 2.61 (2.79). ^1H NMR (CD_3CN, 300 MHz, 298 K): δ 1.94 (s, 3H, $\mathit{CH_3CN}$), 2.33 (d, 12H, $\mathit{Me}_2PCH_2CH_2P\mathit{Me}_2$), 3.19 (m, $Me_2P\mathit{CH_2CH_2}PMe_2$, 4H). $^{13}C\{^1H\}$ NMR (CD_3CN, 75 MHz, 298 K): δ 10.2 (d, $^1J_{P-C}$ = 29 Hz), 31.5 (d, $^1J_{P-C}$ = 27 Hz). ^{31}P NMR (CD_3CN, 120 MHz, 298 K): δ 90.8 (br).

NMR Detection of $(dppm)BiCl_2(OTf)$. TMSOTf (0.111 g, 0.5 mmol) was added to a light-orange solution of $BiCl_3$ (0.157 g, 0.5 mmol) and dppm (0.197 g, 0.5 mmol) in CD_2Cl_2 (3 mL). A clear, dark-orange solution was obtained upon stirring at room temperature for 30 min. The solution was analyzed by NMR spectroscopy. A parallel experiment with 2 equiv of TMSOTf (0.222 g, 1 mmol) yielded identical NMR spectra. ^1H NMR (CD_2Cl_2, 300 MHz, 298 K): δ 4.97 (t, $^2J_{P-H}$ = 8.7 Hz, 2H), 7.38 (m, 12H), 7.59 (m, 8H). $^{13}C\{^1H\}$ NMR (CD_2Cl_2, 75 MHz, 298 K): δ 25.2 (s), 116.8 (q, CF_3, $^1J_{P-C}$ = 319.8 Hz), 128.8 (t, 4.6 Hz), 129.7 (t, 12.4 Hz), 131.4 (s), 133.7 (t, 6.9 Hz). ^{31}P NMR (CD_2Cl_2, 120 MHz, 298 K): δ 18.6 (br).

NMR Detection of $[(dmpe)_2Pd][(CH_3CN)_2Bi_2Cl_6(OTf)_2]$ (8). K_2PdCl_4 (0.066 g, 0.2 mmol) and **3**(OTf)$_2$ (0.147 g, 0.2 mmol) were combined in a vial. Upon the addition of 1 mL of CH_3CN, a gray suspension was formed immediately, which was allowed to stir for 1 h and then settle. The clear, light-orange supernatant was removed via pipet and the gray solid washed with an additional 1 mL of CH_3CN. The wash was combined with the supernatant, and the clear solution was analyzed by ^{31}P NMR spectroscopy and found to contain only one signal, assigned to the $[dmpe_2Pd]^{2+}$ cation. ^{31}P NMR (CH_3CN_2, 120 MHz, 298 K): δ 38.9 (literature δ 38.3, CD_3NO_2).[46] The identity of the product was confirmed from crystals obtained directly from the NMR aliquot, which were analyzed as **8** by X-ray crystallography. Despite repeated recrystallization attempts, it was not possible to completely remove KOTf from its mixture with **8** and obtain the latter as a pure substance.

■ RESULTS AND DISCUSSION

An equimolar combination of $BiBr_3$ and MeOTf in THF results in exothermic elimination of gaseous MeBr and formation of **1**. The reaction mixture becomes gelatinous over the course of the reaction because of Lewis-acid-catalyzed ring-opening polymerization of THF, which is a well-known mode of reactivity for metals in ethereal solvents.[22] Nevertheless, single crystals of the compound were obtained in 78% yield (isolated crystals) upon recrystallization from 1:1 Et_2O/DCM. The crystalline solid

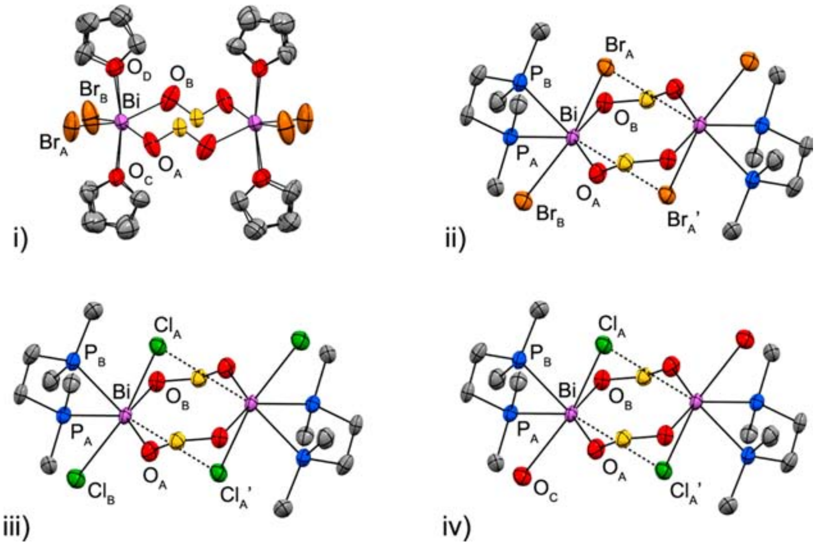

Figure 1. Views of the feature compounds in the solid state (i) **1**, (ii) **2Br**, (iii) **2Cl**, and (iv) **3** showing the geometry at bismuth and interion contacts through the O−S−O moiety of the triflate anions resulting in dimeric association. Thermal ellipsoids are drawn at the 50% probability level. Hydrogen atoms and noninteracting portions of the triflate anions have been omitted for clarity. For facile comparison, the atom labels in this figure are different from those in the CIF files.

Table 1. Selected Solid-State Structural Parameters for Compounds 1, 2Cl, 2Br, and 3 and Related Compounds 4Cl[$\mathrm{BiCl_4}$][23] 4Br[$\mathrm{BiBr_4}$],[24] 5[$\mathrm{SbCl_6}$]$_2$,[37] $\mathrm{THF_3BiBr_3}$,[25] [$\mathrm{Bi_2X_4}$][$\mathrm{AlX_4}$]$_2$ (X = Cl, Br),[26] [$\mathrm{BiCl_2}$][$\mathrm{W_6Cl_{13}}$],[27] and [BiCl][$\mathrm{W_6Cl_{14}}$][28a]

Bi−Cl-Containing Compounds

	2Cl	**3**	**4Cl**[$\mathrm{Bi_2Cl_8}$]$_{0.5}$	[$\mathrm{BiCl_2}$][$\mathrm{W_6Cl_{13}}$]	[$\mathrm{Bi_2Cl_4}$][$\mathrm{AlCl_4}$]$_2$	[$\mathrm{BiCl_2}$]$^+$	**5**[$\mathrm{SbCl_6}$]$_2$	[BiCl][$\mathrm{W_6Cl_{14}}$]	[BiCl]$^{2+}$
P/O−Bi	2.6754(9) $\mathrm{P_A}$	2.6730(10) $\mathrm{P_A}$							
	2.6634(10) $\mathrm{P_B}$	2.6671(12) $\mathrm{P_B}$							
	[2.680]	[2.709]							
		[2.689]							
P−Bi−P	77.95(3)	77.15(3)							
	[80.5]	[79.3]							
Bi−Cl	2.6802(10) $\mathrm{Cl_A}$	2.4990(22)	2.501(6)	2.441(4)	2.392(2)	[2.360]	2.479(6)	2.489(3)	[2.276]
	2.6348(10) $\mathrm{Cl_B}$			2.459(3)	2.663(2)				
	3.623 $\mathrm{Cl_A'}$ [2.626]	[2.435]			2.671(2)				
Cl−Bi−Cl	168.77(3)		91.0(2)	91.38	77.95(6)	[100.0]			
					93.99(9)				
	[155.3]				102.06(6)				
Bi---O	3.010(3) $\mathrm{O_A}$	2.858(4) $\mathrm{O_B}$							
	2.844(2) $\mathrm{O_B}$	2.645(3) $\mathrm{O_C}$							
		2.744(4) $\mathrm{O_A}$							

Bi−Br-Containing Compounds

	1	**2Br**	**4Br**[$\mathrm{BiBr_4}$]	$\mathrm{THF_3BiBr_3}$	[$\mathrm{THFBiBrPh_2}$]	[$\mathrm{THFBiBr_2Ph}$]$_x$	[$\mathrm{Bi_2Br_4}$][$\mathrm{AlBr_4}$]$_2$	[$\mathrm{BiBr_2}$]$^+$	$\mathrm{BiBr_3}$
P/O−Bi	2.4059(5) $\mathrm{O_C}$	2.6883(14) $\mathrm{P_A}$	2.62(9)	2.635(7)	2.589(7)	2.671(8)			
	2.4070(5) $\mathrm{O_D}$	2.6750(13) $\mathrm{P_B}$		2.700(7)					
	[2.382]	[2.690]		2.600(8)					
P/O−Bi−P/O	158.5(5) $\mathrm{O_C}$−Bi−$\mathrm{O_D}$	77.97(4)		90.6(3)					
				85.4(2)					
	[174.1]	[79.9]		89.7(2)					
Bi−Br	2.6068(17) $\mathrm{Br_A}$	2.8332(6) $\mathrm{Br_A}$	2.666(5)	2.628(5)	2.741(1)	2.684(1)	2.555(1)	[2.506]	2.636(4)
	2.6073(17) $\mathrm{Br_B}$	2.7871(6) $\mathrm{Br_B}$		2.6834(13)			2.779(1)		2.660(3)
	[2.579]	3.625 $\mathrm{Br_A'}$ [2.778]		2.6623(11)			2.859(1)		2.692(3)
Br−Bi−Br	93.73(6)	168.09(2)	92.4(1)	92.0(2)			89.41(4)	[101.4]	88.19(10)
				92.6(6)			95.36(4)		90.08(11)
	[100.4]	[162.3]		95.45(5)					96.29(11)
Bi---O	2.7862(5) $\mathrm{O_A}$	2.995(4) $\mathrm{O_A}$							
	2.8299(7) $\mathrm{O_B}$	2.838(4) $\mathrm{O_B}$							

[a] Calculated values in square brackets are for the gas-phase, triflate-free cations at the MP2 level.[29]

retains THF under vacuum (5×10^{-2} mbar) at room temperature, as confirmed by NMR spectroscopy and elemental analysis data. When the crystals are heated under vacuum, an insoluble dark-brown powder is formed.

The reaction of **1** with dmpe in toluene results in quantitative (as shown by ^{31}P NMR spectra of the reaction mixtures) formation of **2Br** with displacement of THF by the chelating ligand. Crystals of **2Br**·CH_3CN were obtained by recrystallization from CH_3CN at −30 °C, but solutions at room temperature deposit black insoluble powder within days. Isolated crystals of **2Br**·CH_3CN are thermally stable under an inert atmosphere at room temperature for weeks.

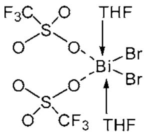

1

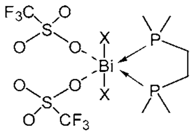

2Cl: X = Cl
2Br: X = Br

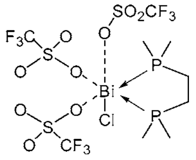

3

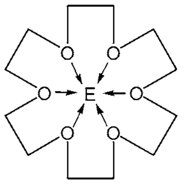

4Cl E = $[BiCl_2][BiCl_4]$
4Br E = $[BiBr_2][BiBr_4]$
5 E = $[BiCl][SbCl_6]_2$

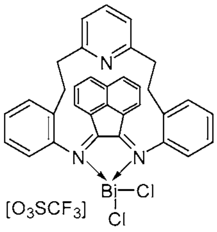

6

Attempts to isolate $(THF)_2BiCl_2(OTf)$ from $BiCl_3$ and MeOTf in THF were unsuccessful because of the rapid thickening of the solvent, suggesting that $BiCl_2^+$ is a more potent polymerization catalyst than $BiBr_2^+$. Therefore, **2Cl** was prepared directly from equimolar mixtures of $BiCl_3$, TMSOTf, and dmpe in toluene and precipitated as an insoluble yellow powder. When $BiCl_3$ was reacted with dmpe in the presence of excess TMSOTf, **3** was obtained. Single crystals of each compound were obtained by recrystallization from CH_3CN at −30 °C because both compounds exhibit thermal instability in solution at room temperature, as judged by the deposition of elemental bismuth within hours. Both compounds are thermally stable for weeks in the solid state under an inert atmosphere.

The solid-state structures of **1**, **2Cl**, **2Br**, and **3** (Figure 1) all involve dimeric arrangements by virtue of Bi---O_{OTf} contacts, which provide two O−S−O bridges between two bismuth centers. The distorted octahedral environment at bismuth is more regular in **1** than in the structures of **2Cl**, **2Br**, and **3**, in which the axially configured halide centers are slanted to accommodate long intermolecular Bi---Cl contacts. The geometry at bismuth in each structure shows no evidence of lone-pair stereochemical activity. Selected structural parameters for each compound are summarized in Table 1 together with analogous parameters for some related compounds.

The structure of **1** is at low resolution because of disorder but is consistent with elemental analysis data and is sufficient to illustrate the connectivity as a cis-configured dibromobismuth center with two trans-configured THF ligands and two cis-configured contacts to oxygen atoms of separate triflate anions. In contrast, the solid-state structures of compounds **2Cl** and **2Br** involve trans-configured halide substituents imposed by the chelating (cis-configured) dmpe ligand. Compound **3** features a bismuth center with a chelating dmpe ligand, one chlorine substituent, and three cis-configured interion contacts to oxygen atoms of separate triflate anions.

The range of Bi---O_{OTf} distances in compounds **1**, **2Cl**, **2Br**, and **3** [2.645(3)−3.010(3) Å] is significantly longer than the sum of the covalent radii [Bi−O = 2.25 Å] and significantly shorter than the sum of the van der Waals radii [Bi---O = 3.80 Å]. While the structure of $Bi(OTf)_3$ has not been reported, the observed Bi---O_{OTf} distances are generally consistent with those reported for representative bismuth triflate compounds [2.473(5)−3.553(6) Å in $Ph_2Bi(OTf)$,[30] 2.386(11)−2.879(15) Å in $(THF)_4ClBi(OTf)_2$,[31] and 2.54(5)−2.84(3) Å in $(H_2O)_4Bi(OTf)_3$[32]] and are generally longer than the Bi−O distances in the covalent oxide α-Bi_2O_3 [2.08(3)−2.80(2) and 3.25(4) Å][33] or alkoxide $Bi(OCPh_3)_3$ [2.070(4)−2.081(4) Å].[34] We conclude that while the Bi---O_{OTf} distances in compounds **1**, **2Cl**, **2Br**), and **3** are generally longer than a formal covalent Bi−O bond, the compounds are best formulated as pseudohalide complexes of the type $[L_2BiX_n(OTf)_{3-n}]_2$ rather than ionic salts of the type $[L_2BiX_n]_2[OTf]_{2(3-n)}$.

To further assess the structural influences of the Bi---triflate interion contacts, we performed ab initio calculations (MP2)[29] to obtain the gas-phase structures of the triflate-free cations of **1**, **2Br**, **2Cl**, and **3** (see Table 1, values in square brackets). The optimized geometry at the bismuth center in the cations of **1**, **2Br**, and **2Cl** is a distorted seesaw, consistent with a AX_4E VSEPR geometry with a stereochemically active lone pair. Further evidence of lone-pair activity in the gas-phase structures comes from the observation that the halide substituents in the cations of **2Br** and **2Cl** are bent back toward the dmpe ligands (Br−Bi−Br = 162.3°; Cl−Bi−Cl = 155.3°) and the THF ligands in the cation of **1** (O−Bi−O = 174.1°) are bent back toward the bromide substituents. The corresponding experimental values for the X−Bi−X bond angle [168.09(2)° for **2Br** and 168.77(3)° for **2Cl**] or the O−Bi−O bond angle [158.5(5)° for **1**(OTf)] are significantly larger than those of the cations in the gas phase, consistent with reduced lone-pair stereochemical activity in the solid state. We did not observe gas-phase minima for the hypothetical tetrahedral geometries for the cations in **1**, **2Br**, and **2Cl** (AX_4 VSEPR). By comparison, a tetrahedral geometry was calculated and observed in the solid state[39] for the recently reported $[(Me_3P)_2SnCl_2]^{2+}$ dication, consistent with an AX_4 VSEPR geometry. The *trans*-THF_2 structure observed for the cation in the solid-state structure of **1** is calculated to be a minimum for the cation of **1** in the gas phase, while there is no minimum evident for the hypothetical *cis*-THF_2 structure with *trans*-bromine substituents. The calculated P−Bi bond lengths and angles for the cations of **2Br**, **2Cl**, and **3** are very similar to those observed in the solid state, while the calculated Bi−X (X = Cl or Br) bonds are significantly shorter than those observed in the solid state. We conclude that interactions with the triflate ion suppress the lone-pair stereochemical activity at bismuth and attenuate the overall Lewis acidity of the metal centers in the solid state, leading to lengthened Bi−X bonds.

In the solid state, the cis Bi−Br bonds in **1** [Br−Bi−Br = 93.73(6)°] are shorter than those in **4Br**, $(THF)_3BiBr_3$, $BiBr_3$, $(THF)BiPh_2Br$, and $[(THF)BiPhBr_2]_x$ and are similar to those in $[Bi_2Br_6][AlBr_4]_2$, all of which feature cis Bi−Br bonds. The trans configuration of bromine atoms in **2Br** is accompanied by substantially longer Bi−Br bonds, likely because of a trans influence, which is also predicted by the MP2-optimized structure of the cation of **2Br** in the gas phase. Consistently, the

Table 2. Crystal Data for the Featured Compounds

	1	**2Br**·CH_3CN	**2Cl**·CH_3CN	**3**·CH_3CN	**8**
empirical formula	$C_9H_{16}BiBr_2SO_5F_3$	$C_9H_{19}BiBr_2F_3O_3P_2SN$	$C_9H_{19}BiCl_2F_3NO3P2S$	$C_{10}H_{19}BiClF_6NO_6P_2S2$	$C_{18}H_{38}Bi_2Cl_6F_6N_2O_6P_4PdS_2$
fw	662.08	709.05	620.13	733.75	1417.56
space group	$P\bar{1}$	$C2/c$	$C2/c$	$P2(1)/n$	$P\bar{1}$
a (Å)	8.088(2)	21.1892(16)	21.2850(16)	12.6020(15)	8.9289(4)
b (Å)	10.539(4)	15.3454(16)	15.2439(16)	16.2877(19)	9.8177(4)
c (Å)	11.746(3)	12.6533(11)	12.3056(10)	12.8527(15)	13.9674(6)
α (deg)	106.091(5)	90	90	90	106.6802(4)
β (deg)	97.960(4)	94.694(2)	95.629(2)	118.648(1)	94.1676(5)
γ (deg)	106.559(3)	90	90	90	107.2454(5)
V (Å^3)	896.1(4)	4100.5(6)	3973.5(6)	2315.2(5)	1103.37
Z	2	8	8	4	1
ρ (g cm^{-3})	2.454	2.297	2.073	2.105	2.133
λ (Å)	0.71073	0.71073	0.71073	0.71073	0.71073
T (K)	188(1)	198(1)	198(1)	173(1)	173
GOF	1.048	1.032	1.037	1.058	1.106
R1[a]	0.0498	0.0397	0.0274	0.0320	0.0136
wR2[a]	0.1222	0.0922	0.0583	0.0663	0.0331

[a] $R1 = \sum||F_o| - |F_c||/\sum|F_o|$. $wR2 = [\sum w(F_o^2 - F_c^2)^2/\sum w(F_o^4)]^{1/2}$.

trans-configured Bi–Cl bonds [Cl–Bi–Cl = 168.77(3)°] in **2Cl** are also significantly longer than those in related species, including neutral $BiCl_3$ [2.500(18) Å][35] and **6** [2.5116(8) and 2.5269(8) Å],[36] which feature a cis configuration of chlorine centers at the bismuth center. As expected, the Bi–Cl bond in **3** [2.4990(22) Å] is markedly shorter than that in **2Cl** and is only marginally longer than those observed in the related **5** [2.479(6) Å][37] and $[BiCl][W_6Cl_{14}]$ [2.489(3) Å].[28] By comparison, the shortest Bi–Cl bond reported in the Cambridge Structural Database to date is 2.394 Å in the neutral arene complex (p-xylene)$_2Bi_2Cl_6$,[38] and the MP2-optimized value for the hypothetical gas-phase diatomic $[BiCl]^{2+}$ is 2.276 Å.

The observed and calculated P–Bi bond lengths in **2Br**, **2Cl**, and **3** are essentially equivalent, suggesting that these are insensitive to the Lewis acidity of the bismuth center, despite the greater electronegativity of the chlorine substituents and the greater charge in **3**. Moreover, the P–Bi bond lengths in **2Cl** and **2Br** are similar to those in neutral and anionic compounds containing P–Bi bonds (Table 1). Therefore, the substantially shorter Bi–Cl and Bi---O_{OTf} distances in **3** compared to those in **2Cl** preferentially compensate for the enhanced Lewis acidity at the metal center. The differing sensitivity of the E–X and E–P bonds to the charge at the metal center is consistent with observations for cationic P–SbX_n and P–SnX_n complexes and may be a general feature of phosphine complexes of main-group halides.[3,39] The Lewis basicity and configuration of the phosphine ligands is, nevertheless, important. Thus, the more basic dmpe ligand results in substantially shorter P–Bi distances than those found in $[(Ph_3P)_2BiPh_2][PF_6]$ [2.968(3) and 2.937(3) Å],[6] which bears trans-configured phosphine ligands.

The Bi–O_{THF} lengths in **1** are approximately 0.23 Å shorter than those in the neutral adducts $(THF)_3BiBr_3$, $(THF)BiPh_2Br$, or polymeric $[(THF)BiPhBr_2]_x$, reflecting a stronger Bi–O_{THF} interaction in the triflate complex despite the trans configuration of the ether ligands. Taken together with the short Bi–Br bonds in **1** (vide supra), these features demonstrate that the bismuth center in this complex is highly Lewis acidic even in the presence of the triflate contacts.

The structure of **2Cl** is consistent with that of the antimony derivative $[(dmpe)SbCl_2][OTf]$ (**7**)[3] with trans-configured chlorine substituents imposed by the stereochemically active lone pair. While the average E–Cl and E–P bond lengths [2.6678(20) and 2.6694(19) Å, respectively] are predictably longer in **2Cl** than in **7** [2.5625(8) and 2.5657(8) Å, respectively] because of the larger covalent radius of bismuth (1.48 Å, compared to that of antimony at 1.39 Å), the average of two contacts to the triflate anions are ca. 0.05 Å shorter for **2Cl** [2.927(5) Å] than for **7** [2.9746(28) Å], because of the lesser steric restriction at the larger bismuth atom and the lower stereochemical activity of the Bi 6s lone pair compared to the 5s lone pair in **7**. In this context, the dimeric structure adopted by **2Cl** is not observed for **7**, which adopts a complex network structure where the two interacting triflate anions bridge different metal centers in the extended solid-state structure (Table 2).[3]

Recently, it has been shown that, because of the combination of low-lying vacant acceptor orbitals and a lone pair at the central phosphorus atom, ligands of the type $[LPR_2]^+$ and $[L_3P]^{3+}$ (L = carbene) can coordinate with electron-rich late transition metals,[40] classifying these main-group cations as a novel family of π-accepting ligands with demonstrated applications in catalysis.[41] Transition-metal complexes bearing cationic ligands of the type $[R_3P{-}P{-}PR_3]^+$ have also been characterized by NMR spectroscopy.[42] However, despite the well-established use of neutral stibine and bismuthine[43] ligands in transition-metal chemistry, investigations of their Z-type ligand abilities are limited. Only two instances of well-established bismuth–metal coordinate bonds have been reported, both employing P–Bi–P-type pincer ligands to bind gold(I) in a tridentate fashion, such that the P–Au interaction assists in enforcing the Au–Bi interaction.[44a,b] Analysis of the bonding situation showed that in both cases the Au–Bi bonding was driven by transfer of the electron density from the gold atom to the Bi–Cl σ^* antibonding orbital. Fernandez et al. have also reported a long Bi–Au [3.7284(5) Å] interaction between the cation $[Bi(C_6H_4CH_2NMe_2\text{-}2)_2]^+$ and the anion $[Au(C_6F_5)_2]^-$, without the need for a pincer framework or other structure-directing features to enforce the Bi–Au contact.[45]

Following an analysis of the electronic structure of **3** at the MP2 level, we reasoned that, analogous to the cases above, the low-lying vacant p-orbitals centered at the bismuth atom in **3** (Figure 2a) may also serve as π-acceptor orbitals with electron-rich, late-transition-metal donors, enhanced by localization of the highest occupied molecular orbital (HOMO) on the bismuth atom (Figure 2b), prompting an assessment of the σ-donor/π-acceptor ligand capabilities of **3**.

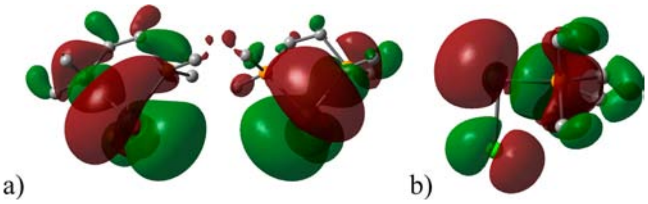

Figure 2. Surface plots (|isovalue| = 0.02) of (a) $\mathbf{3}_{\text{LUMO}}$ (−9.63 eV) and $\mathbf{3}_{\text{LUMO+1}}$ (−9.74 eV) and (b) $\mathbf{3}_{\text{HOMO}}$ (−18.12 eV).

The addition of a CH_3CN solution of $\mathbf{3}(OTf)_2$ to 1 equiv of K_2PdCl_4 results in the formation of a clear orange solution, which shows a single peak at δ 38.9 in the ^{31}P NMR spectrum of the reaction mixture, consistent with formation of the known $[dmpe_2Pd]^{2+}$ cation.[46] Concentration of the solution under vacuum yields a large quantity of light-gray powder and crystalline blocks. The identity of the crystalline material was confirmed by X-ray crystallography to be **8** (Figure 3). The gray powder showed no signals in its ^1H or ^{31}P NMR spectrum, consistent with its formulation as a mixture of KOTf and unreacted K_2PdCl_4, implying the overall reaction shown in Scheme 1.

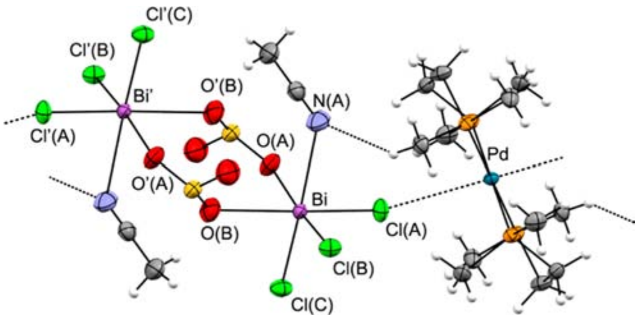

Figure 3. View of the solid-state structure of **8**. Thermal ellipsoids are drawn at the 30% probability level. Noninteracting portions of the triflate anion have been omitted. The anion $[(CH_3CN)_2Bi_2Cl_6(OTf)_2]^{2-}$ is centrosymmetric. Select bond lengths (Å) and angles (deg) are as follows: Bi−Cl(A) = 2.5074(6), Bi−Cl(B) = 2.5192(6), Bi−Cl(C) = 2.5171(6), Bi−O(A) = 2.6617(18), Bi−O(B) = 2.6724(18), Bi−N1 = 2.757(2); Cl(A)−Bi−Cl(B) = 94.400(19), O(A)−Bi−O(B) = 84.30(6), O(A)−Bi−Cl(B) = 171.49(6), O(B)−Bi−Cl(A) = 172.14(5), N(A)−Bi−Cl(C) = 171.49(6). For facile comparison, the atom labels in this figure are different from those in the CIF file.

The $[Bi_2Cl_8]^{2-}$ dianion is a well-known formulation that is observed as dimers,[23] a polymer,[47] and ligand-supported dimers.[48−50] The last of these best describes $[(CH_3CN)_2Bi_2Cl_6(OTf)_2]^{2-}$, which crystallizes as a centrosymmetric edge-sharing bioctahedron via two O−S−O linkages between adjacent bismuth centers. The preference for phosphine/halide exchange (metathesis) over Bi−Pd Z-type coordination evidences a substantially higher Lewis acidity at the bismuth center in $\mathbf{3}(OTf)_2$ (p-orbitals as acceptor molecular orbitals) than in the formally more highly charged phosphorus-centered cations (p-orbital-derived acceptor molecular orbitals) or in the neutral halobismuthines (Bi−X σ^*-acceptor molecular orbitals). Moreover, whereas the 3s lone pair in cationic phosphines readily engages the transition metal, leading to synergistic σ donation and π back-donation, the contracted 6s lone pair at the bismuth center in **3** is a much weaker Lewis base and likely does not benefit from such an interaction. It is therefore unlikely that bismuth complexes such as **3** can be used as ligands in the absence of additional structure-enforcing factors such as pincer chelation.

■ CONCLUSIONS

In summary, the synthesis and characterization of compounds featuring bismuth acceptors stabilized by THF or dmpe ligands are described. In the solid state, the triflate-containing compounds **1**, **2Br**, **2Cl**, and **3** crystallize as dimers involving Bi---O_{OTf} and Bi---X interactions. The Bi−X bond lengths exhibit a greater sensitivity to the formal Lewis acidity of the bismuth center than do the Bi−P bond lengths. The strong trans influence of the halide ligands is also documented. A comparison of homologous Sb/Bi structures **2Cl** and **7** illustrates the structural consequences of relative lone-pair stereochemical activity. In solution, the compounds behave as classic coordination complexes, as illustrated by the ligand substitution reaction that yields **2Br** from a solution of **1** with dmpe. An assessment of the electronic structure of **3** suggests that it may behave as a Z-type ligand because of the presence of both a lone pair and vacant p orbitals at the bismuth center. However, experimental attempts to realize such reactivity were unsuccessful and led instead to the discovery of a metathesis reaction highlighting an important distinction between the chemistry of phosphorus and bismuth cations, with the latter showing a substantially greater Lewis acidity even with lower formal charges and more strongly interacting counterions. These insights provide direction for the further development and diversification of the coordination chemistry of bismuth.

■ ASSOCIATED CONTENT

Ⓢ Supporting Information

Cartesian coordinates for gas-phase-optimized compounds and CIF files. This material is available free of charge via the Internet at http://pubs.acs.org.

■ AUTHOR INFORMATION

Corresponding Author

*E-mail: nburford@uvic.ca. Phone: +1 250 721 7150.

Notes

The authors declare no competing financial interest.

Scheme 1. Reaction between 3 and K_2PdCl_4

$$[dmpeBiCl(OTf)_2] + K_2PdCl_4 \xrightarrow{\times} [dmpeBi(Cl)PdCl_4] + 2KOTf$$

$$2[dmpeBiCl(OTf)_2] + K_2PdCl_4 + 2CH_3CN \longrightarrow [dmpe_2Pd][(CH_3CN)_2Bi_2Cl_6(OTf)_2] + 2KOTf$$

■ ACKNOWLEDGMENTS

The authors gratefully acknowledge the Natural Sciences and Engineering Council of Canada for financial support and the Vanier Canada Graduate Scholarships Program for a graduate scholarship (to S.S.C.).

■ REFERENCES

(1) Dyker, C. A.; Burford, N. *Chem.—Asian J.* **2008**, *3*, 28−36.

(2) Conrad, E.; Burford, N.; Werner-Zwanziger, U.; McDonald, R.; Ferguson, M. *Chem. Commun.* **2010**, *46*, 2465−2467.

(3) Chitnis, S.; Peters, B.; Conrad, E.; Burford, N.; McDonald, R.; Ferguson, M. *Chem. Commun.* **2011**, *47*, 12331−12333.

(4) Wielandt, J. W.; Kilah, N. L.; Willis, A. C.; Wild, S. B. *Chem. Commun.* **2006**, 3679−3680.

(5) Chitnis, S. S.; Carpenter, Y.-Y.; Burford, N.; McDonald, R.; Ferguson, M. J. *Angew. Chem., Int. Ed.*, **2013**, *52*, 4863−4866

(6) Kilah, N. L.; Petrie, S.; Stranger, R.; Wielandt, J. W.; Willis, A. C.; Wild, S. B. *Organometallics* **2007**, *26*, 6106−6113.

(7) Conrad, E.; Burford, N.; McDonald, R.; Ferguson, M. J. *Chem. Commun.* **2010**, *46*, 4598−4600.

(8) Rat, C. I.; Silvestru, C.; Breunig, H. J. *Coord. Chem. Rev.* **2013**, *257*, 818−879.

(9) Silvestru, C.; Breunig, H. J.; Althaus, H. *Chem. Rev.* **1999**, *99* (11), 3277−3328.

(10) Clegg, W.; Elsegood, M. R. J.; Graham, V.; Norman, N. C.; Pickett, N. L.; Tavakkoli, K. *J. Chem. Soc., Dalton Trans.* **1994**, 1743−1751.

(11) Willey, G. R.; Daly, L. T.; Drew, M. G. B. *J. Chem. Soc., Dalton Trans.* **1996**, 1063−1067.

(12) Genge, A. R. J.; Hill, N. J.; Levason, W.; Reid, G. *Dalton Trans.* **2001**, 1007−1012.

(13) Hockless, D. C. R.; Norman, N. C. *Chem. Ber.* **1991**, *124*, 2457−2459.

(14) Clegg, W.; Elsegood, M. R. J.; Graham, V. *J. Chem. Soc., Dalton Trans.* **1993**, 997−998.

(15) Clegg, W.; Elsegood, M. R. J.; Norman, N. C.; Pickett, N. L. *J. Chem. Soc., Dalton Trans.* **1994**, 1753−1757.

(16) Petuškova, J.; Bruns, H.; Alcarazo, M. *Angew. Chem., Int. Ed.* **2011**, *50*, 3799−3802.

(17) Petuškova, J.; Patil, M.; Holle, S.; Lehmann, C. W.; Thiel, W.; Alcarazo, M. *J. Am. Chem. Soc.* **2011**, *133* (51), 20758−20760.

(18) Carreras, J.; Patil, M.; Thield, W.; Alcarazo, M. *J. Am. Chem. Soc.* **2012**, *134* (40), 16753−16758.

(19) Frisch, M. J.; Trucks, G. W.; Schlegel, H. B.; Scuseria, G. E.; Robb, M. A.; Cheeseman, J. R.; Scalmani, G.; Barone, V.; Mennucci, B.; Petersson, G. A.; Nakatsuji, H.; Caricato, M.; Li, X.; Hratchian, H. P.; Izmaylov, A. F.; Bloino, J.; Zheng, G.; Sonnenberg, J. L.; Hada, M.; Ehara, M.; Toyota, K.; Fukuda, R.; Hasegawa, J.; Ishida, M.; Nakajima, T.; Honda, Y.; Kitao, O.; Nakai, H.; Vreven, T.; Montgomery, J. A., Jr.; Peralta, J. E.; Ogliaro, F.; Bearpark, M.; Heyd, J. J.; Brothers, E.; Kudin, K. N.; Staroverov, V. N.; Kobayashi, R.; Normand, J.; Raghavachari, K.; Rendell, A.; Burant, J. C.; Iyengar, S. S.; Tomasi, J.; Cossi, M.; Rega, N.; Millam, J. M.; Klene, M.; Knox, J. E.; Cross, J. B.; Bakken, V.; Adamo, C.; Jaramillo, J.; Gomperts, R.; Stratmann, R. E.; Yazyev, O.; Austin, A. J.; Cammi, R.; Pomelli, C.; Ochterski, J. W.; Martin, R. L.; Morokuma, K.; Zakrzewski, V. G.; Voth, G. A.; Salvador, P.; Dannenberg, J. J.; Dapprich, S.; Daniels, A. D.; Farkas, Ö.; Foresman, J. B.; Ortiz, J. V.; Cioslowski, J.; Fox, D. J. *Gaussian 09*, revision A.1; Gaussian, Inc.: Wallingford, CT, 2009.

(20) Peterson, K. A.; Yousaf, K. E. *J. Chem. Phys.* **2010**, *133*, 174116−36.

(21) Metz, B.; Stoll, H.; Dolg, M. *J. Chem. Phys.* **2000**, *113*, 2563−2569.

(22) Woodhouse, M. E.; Lewis, F. D.; Marks, T. J. *J. Am. Chem. Soc.* **1982**, *104*, 5586−5594.

(23) Alcock, N. W.; Ravindran, M.; Willey, G. R. *J. Chem. Soc., Chem. Commun.* **1989**, 1063.

(24) Rogers, R. D.; Bond, A. H.; Aguinaga, S.; Reyes, A. *J. Am. Chem. Soc.* **1992**, *114*, 2967−2977.

(25) Carmalt, C. J.; Clegg, W.; Elsegood, M. R. J.; Errington, R. J.; Havelock, J.; Lightfoot, P.; Norman and, N. C.; Scott, A. J. *Inorg. Chem.* **1996**, *35*, 3709−3712.

(26) Beck, J.; Hengstmann, M.; Schlüter, S. *Z. Kristallogr.* **2005**, *220*, 147−151.

(27) Ströbele, M.; Meyer, H. J. *Z. Anorg. Allg. Chem.* **2009**, *635* (11), 1517−1519.

(28) Ströbele, M.; Jüstel, T.; Bettentrup, H.; Meyer, H. J. *Z. Anorg. Allg. Chem.* **2009**, *635*, 822−827.

(29) See the Supporting Information for Cartesian coordinates of optimized structures.

(30) Beckmann, J.; Bolsinger, J.; Duthie, A.; Finke, P.; Lork, E.; Lüdtke, C.; Mallow, O.; Mebs, S. *Inorg. Chem.* **2012**, *51*, 12395−12406.

(31) Mazières, S.; Le Roux, C.; Peyronneau, M.; Gornitzka, H.; Rocques, N. *Eur. J. Inorg. Chem.* **2004**, *14*, 2823−2826.

(32) Louër, M. *Chem. Mater.* **1997**, *9*, 3012−3016.

(33) Malmros, G. *Acta Chem. Scand.* **1970**, *24*, 384−396.

(34) Hanna, T. A.; Keitany, G.; Ibarra, C.; Sommer, R. D.; Rheingold, A. L. *Polyhedron* **2001**, *20*, 2451−2455.

(35) Nyburg, S. C.; Ozin, G. A.; Szymanski, J. T. *Acta Crystallogr., Sect. B* **1971**, *27*, 2298−2304.

(36) Brazeau, A. L; Jones, N. D.; Ragogna, P. J. *J. Chem. Soc., Dalton Trans.* **2012**, *41*, 7890−7896.

(37) Schäfer, M.; Frenzen, G.; Neumüller, B.; Dehnicke, K. *Angew. Chem., Int. Ed.* **1992**, *31*, 334−335.

(38) Muller-Beck, S.; Frank, W.; Schneider, J. *Z. Anorg. Allg. Chem.* **1993**, *619*, 1073−1082.

(39) MacDonald, E.; Doyle, L.; Chitnis, S. S.; Werner-Zwanziger, U.; Burford, N.; Decken, A. *Chem. Commun.* **2012**, *48*, 7922.

(40) Petuškova, J.; Patil, M.; Holle, S.; Lehmann, C. W.; Thiel, W.; Alcarazo, M. *J. Am. Chem. Soc.* **2011**, *133* (51), 20758−20760.

(41) Carreras, J.; Patil, M.; Thield, W.; Alcarazo, M. *J. Am. Chem. Soc.* **2012**, *134* (40), 16753−16758.

(42) Coffer, P. K.; Deng, R. M. K.; Dillon, K. B.; Fox, M. A.; Olivey, R. J. *Inorg. Chem.* **2012**, *51*, 9799−9808.

(43) Braunschweig, H.; Cogswell, P.; Schwab, K. *Coord. Chem. Rev.* **2011**, *255*, 101−117.

(44) (a) Tsersich, C.; Limberg, C.; Roggan, S.; Herwig, C.; Ernsting, N.; Kovalenko, S.; Mebs, S. *Angew. Chem., Int. Ed.* **2012**, *51*, 4989−4992. (b) Lin, T.; Ke, I.; Gabbai, F. P. *Angew. Chem., Int. Ed.* **2012**, *51*, 4985−4988.

(45) Fernandez, E. J.; Laguna, A.; Lopez-de-Luzuriaga, J. M.; Monge, M.; Nema, M.; Olmos, M. E.; Perez, J.; Silvestru, C. *Chem. Commun.* **2007**, 571−573.

(46) Berning, D. E.; Noll, B. C.; DuBois, D. L. *J. Am. Chem. Soc.* **1999**, *121* (49), 11432−11447.

(47) Kushch, N. D.; Dyachenko, O. A.; Gritsenko, V. V.; Cassoux, P.; Faulmann, C.; Kobayashi, A.; Kobayashi, H. *J. Chem. Soc., Dalton Trans.* **1998**, 683−688.

(48) Breunig, H. J.; Denker, M.; Schulz, R. E.; Lork, E. *Z. Anorg. Allg. Chem.* **1998**, *624*, 81−84.

(49) Ahmed, I. A.; Blachnik, R.; Reuter, H. *Z. Anorg. Allg. Chem.* **2001**, *627*, 2057−2062.

(50) Yu, Y.; Qian, K.; Ye, Y. *J. Mol. Struct.* **2012**, *1021*, 1−6.